Mangiferin Enhances the Therapeutic Efficacy of Bone Marrow Mesenchymal Stem Cells on Cyclophosphamide-Induced Cardiac Toxicity in Adult Male Albino Rat Models

Mai Hassan Ibrahim[1], Rasha M. Salama[2]

KEYWORDS
Cyclophosphamide,
Cardiotoxicity,
Mangiferin,
BM-MSCs,
CK-MB.

ABSTRACT

Between 7 and 28% of patients receiving cyclophosphamide (CP) have cardiotoxicity. This study looked to learn more about the enhancement effects of Mangiferin on the therapeutic efficacy of bone marrow mesenchymal stem cells (BM-MSCs) on CP-induced cardiac toxicity in adult rat models. Ninety male albino rats were separated into six groups: control, CP, withdrawal, CP plus Mangiferin, CP plus BM-MSCs, and CP plus Mangiferin and BM-MSCs groups. When the cardiac muscle of the CP group was examined under a microscope, the cardiac muscle fibers were vacuolated, and there was mononuclear infiltration between the fibers. Also, myofibril disintegration, enlarged, dilated SER, and degenerated mitochondria were observed ultra-structurally. Some nuclei had chromatolysis, whereas others were heterochromatic with irregular nuclear membranes. These outcomes were validated by a highly significant increase in α-SMA and a highly significant decrease in Bcl-2, as well as increased collagen fiber deposition, additionally confirmed by biochemical results in the form of elevated serum levels of CK-MB and LDH and tissue MDA levels. The withdrawal group's outcomes resembled those of the CP group. The CP plus Mangiferin group and CP plus BM-MSCs groups improved cardiac muscle architecture, collagen fiber deposition, serum levels of CK-MB, LDH, and tissue MDA levels, but still did not achieve complete improvement in histological, ultrastructural, Immunohistochemical, and biochemical cardiac parameters. Lately, the CP plus Mangiferin and BM-MSCs group produced results closely similar to the control group.

Introduction

Cyclophosphamide (CP) is an alkylating, oxazaphosphorine-substituted nitrogen mustard anticancer medication for lymphoma, myeloma, and leukemia (Katayama et al., 2009) that exhibits significant cytotoxic and immunosuppressive action (Kim and Chan, 2017).

Between 7 and 28% of patients receiving CP had cardiotoxicity (Iqubal et al., 2019). It is dose-dependent, with early, abrupt, fatal onset occurring 2 to 3 weeks after intake of 180 to 200 mg CP (Bhatt et al., 2017).

Cells of endothelium are more vulnerable to CP-induced damage than other cells due to their high rate of proliferation (Ranchoux et al., 2015).

Generally, oxidative and nutritive stress that induces cardiomyocyte inflammation, converted calcium homeostasis, cell death, enlarged cardiomyocytes, split nuclei, vacuolization,

[(1)] *Anatomy and Embryology Department, Faculty of Medicine, Benha University, Benha, Egypt.*
[(2)] *Anatomy and Embryology Department, Faculty of Medicine, Menoufia University, Menoufia, Egypt.*
*** Corresponding author:** Mai Hassan Ibrahim
E-mail address: drmayoy11@yahoo.com
Mobile: 01145779734
ORCID: 0000-0001-5999-2612

and changes in signaling pathways are the mechanisms of CP-induced cardiotoxicity (Iqubal et al., 2019).

Multipotent stem cells, known as mesenchymal stem cells (MSCs), can be found in a variety of tissues, including bone marrow, adipose tissue, and umbilical cord blood (Ren et al., 2016). Because of their exceptional biological characteristics, such as their ease of isolation, minimal immunogenicity, and various differentiation potentials, they have received a lot of attention (Liao et al., 2019; Sun et al., 2021).

Mesenchymal stem cells have been used as a permeation therapy to "regrow" lost cardiomyocytes, remedy endogenous tissue, and also be beneficial for the therapy of many heart diseases due to paracrine signaling and displaying novel immunomodulatory properties (Sun et al., 2016). Thereafter, the success of MSCs in cardiac disease has been the cornerstone of research (Afzal et al., 2015).

Bone marrow mesenchymal stem cells (BM-MSCs) have attained favorable attention and progression in the therapeutics of patients with myocardial infarction and ischemic heart failure (Luo et al., 2017). However, the limited clinical efficacy of transplanted BMSCs has restricted their use (Traverse et al., 2011).

Nowadays, natural products are a significant source for designing and creating novel medications that target the cardiovascular system. Many active plant substances have been assured to have an antioxidant effect, hindering the damage caused by free radicals. Mangiferin (2-β-D-glucopyranosyl-1,3,6,7-tetrahydroxy-9H-xanthen-9-one) is a safe, incoming, natural bioactive compound obtained from mango fruits (Mangifera indica Linn) and their by-products (Thomford et al., 2018) and also is a well-known C-glucoside xanthone (Guan et al., 2019) that has many profitable impacts, including anti-oxidative through free radical scavenger and its iron-chelating capabilities, anti-inflammatory, anti-apoptotic, anti-diabetic, and anti-aging actions (Du et al., 2018).

Additionally, several researchers have specified the valuable cardioprotective effects of Mangiferin on the cardiovascular system (Jiang et al., 2020), among them coronary heart diseases, diabetic cardiomyopathy, myocardial ischemia-reperfusion, and cardiac inflammation (Suchal et al., 2017). Also, Mangiferin has several health-endorsing properties, including antineoplastic, antibacterial, antiviral, antiallergic, and immune-modulatory (Sadhukhan et al., 2018; He et al., 2019).

This study sought to explore the enhancement effects of Mangiferin on the therapeutic efficacy of BM-MSCs on CP-induced cardiac toxicity in adult male albino rat model.

Material and Methods

Experimental chemicals

- **Cyclophosphamide, or CP** (End·xan vials; Baxter C·mpany, USA) a vial held 200 mg of CP in the shape of lyophilized, dry p·wder. To create a concentrated solution (20 mg/ml) for rapid injection, the contents of one vial were dissolved in 10 millilitres of normal saline (0.9% NaCl) (Helal et al., 2020).
- **Mangiferin** (C19H18O11; systematic name: 1,3,6,7-tetrahydroxyxanthone C2-ß-D-glucoside) was obtained from Sigma-Aldrich Chemical Company in St. Louis, Missouri, USA, accessible in the form of powder (1 g in glass bottle) at a dose of (100 mg/kg, i.p), and dissolved in 0.5% dimethyl sulfoxide (DMSO) (2 ml/kg/day;

i.p) (Akter et al., 2022). According to Prado et al. (2015), LD50 value reported for mangiferin was 400mg/kg after acute i.p.

Experimental animals

Ninety adult male albino rats (180-200 g/each) were applied in this experiment. Rats were shielded in separate well aerated clean containers, at room temperature and under strict care and hygienic conditions with free use to food and water. The experiment was acted upon in Faculty of Medicine, Benha University. This study was authorized by the Research Ethics C٠mmittee of the related institutes (Rc 51:10.2022).

Experimental protocol

The rats were distributed into the following six experimental groups:

Group I (Control group): that was more classified into four subgroups (10 rats each);

Subgroup Ia (negative c٠ntr٠l): rats were left with no treatments throughout the experiment, and used as donor for BM-MSCs.

Subgroup Ib (positive control 1): rats had one intraperitoneal injection of 2 ml of normal saline (0.9% NaCl) on 1st day of the experiment (vehicle for CP).

Subgroup Ic (positive control 2): rats were injected intraperitoneally with 0.5% DMSO (2 ml/kg/day) from 10th day of the experiment for 10 consecutive days (vehicle for Mangiferin).

Subgroup Id (positive control 3): rats had one intraperitoneal injection of 0.5 ml PBS ٠n 10th day of the experiment (vehicle for BM-MSCs).

Rats of the four subgroups were sacrificed on 30th day of the experiment.

Group II (CP group, n=10): rats received a solitary intraperitoneal injection of CP (200 mg/kg) on 1st day of the experiment and were sacrificed on 10th day of the experiment.

Group III (Withdrawal group, n=10): rats received a solitary intraperitoneal injection of CP (200 mg/kg) on 1st day of the experiment and were sacrificed on 30th day.

Group IV (CP plus Mangiferin group, n=10): rats were injected a solitary intraperitoneal injection of CP (200 mg/kg) on 1st day of the experiment, followed by intraperitoneal injection of Mangiferin (100 mg/kg) dissolved in 0.5% DMSO (2 ml/kg) from 10th day of the experiment for ١٠ consecutive days, then all rats were sacrificed on 30th day.

Group V (CP plus BM-MSCs group, n=10): rats were injected a solitary intraperitoneal injection of CP (200 mg/kg) on 1st day of the experiment, followed by a solitary intraperitoneal dosage of 2×10^6 cells/rat BM-MSCs dissolved in PBS injected on 10th day of the experiment, and were sacrificed on 30th day.

Group VI (CP plus Mangiferin and BM-MSCs group, n=10): rats received a solitary intraperitoneal injection of CP (200 mg/kg) on 1st day of the experiment, followed by intraperitoneal injection of Mangiferin (100 mg/kg) from 10th day of the experiment for 10 consecutive days, and a solitary intraperitoneal injection of 2×10^6 cells/rat BM-MSCs dissolved in PBS on 10th day of the experiment, then rats were sacrificed on 30th day.

Bone marrow mesenchymal stem cells (BM-MSCs)

Preparation of BM-MSCs:

BM-MSCs isolation: The knee area was meticulously shaved and cleaned with 70% ethanol and povidone iodine after the animals were given 60 mg/kg ketamine and 6 mg/kg xylazine intraperitoneally to induce anaesthesia. By rotating, the syringe was inserted into the proximal tibial and distal femoral bone lumens. Next, 0.1 ml of heparin sulphate was mixed with aspirated BM using a syringe. All BM samples were combined with 1ml of full culture medium, which included 15% foetal bovine serum, elevated-glucose Dulbecco's modified eagle medium, 100U/ml penicillin G, and 100U/ml streptomycin (all from Gibco, Paisley, UK). After centrifuging the BM/medium combination at 1200 rpm for 5 minutes, the supernatant was excluded, after that the cellular pellet was resuspended in warm, culture medium in 25 cm2 cell culture flasks and moved to an incubator at 37 °C in a humidified 5% CO2 environment. Every three to four days, the medium was changed, and the cells were subcultured until the development of big colonies, or for 12 to 14 days as a main culture. Cultures were twice washed in PBS after big colonies (80 to 90% confluence) formed, and the cells were then trypsinized for five minutes at 37°C with 0.25% trypsin in 1mL EDTA. Cells were separated by centrifugation (2400 rpm for 20 min) and then resuspended in medium containing serum before being cultured in flasks measuring 25 cm^2. First-passage cultures were the outcome. MSCs in culture can be identified by their fusiform structure and adhesiveness. On day 14, the ability adhering cell clusters' proved that they were MSCs (Short and Wagey, 2013).

Stem Cells Labeling with PKH26 Dye: throughout the 4^{th} passage, MSCs were labeled using PKH26 fluorescent linker dye. Red fluorochrome PKH26 emits light at 567 nm and is excited at 551 nm. Labeled cells maintain both metabolic and proliferative processes. The linker is therefore appropriate for in vitro cell labeling, in vivo cell monitoring, and studies on in vitro cell growth. The dye is stable and will proportionately divide as cells divide. Discovery of injected cells that are homing in the rat's heart: after the scarification of rats of groups V & VI, the rat heart was inspected under a fluorescence microscope to look for cells that were stained with PKH26 dye. These enabled researchers to verify that the cells that had been injected had grafted onto the heart of Groups V and VI, PKH 26-tagged cells have strong red auto-fluorescence (Figure 1).

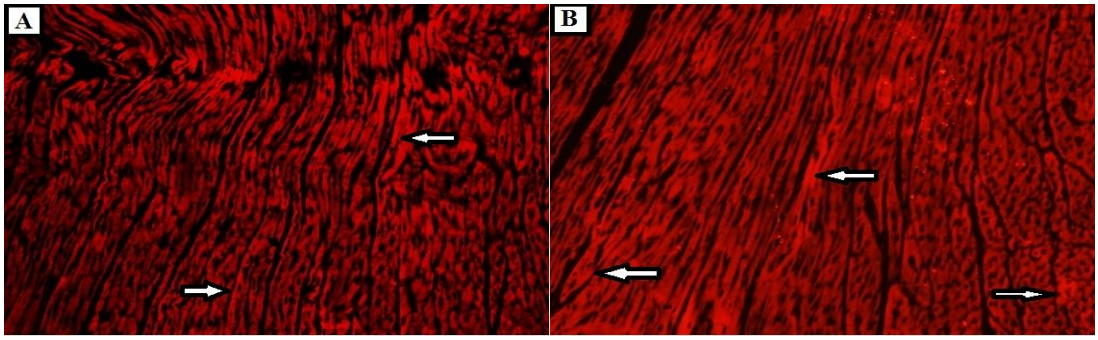

Fig. (1) (A) A photomicrograph of a section of the adult rat heart of CP plus BM-MSCs group exhibiting positive red auto-fluorescence PKH26 fluorescent dye labeled MSCs (arrows). **(B)** A photomicrograph of a section of a rat heart of CP plus Mangiferin and BM-MSCs group viewing positive red auto-fluorescence PKH26 fluorescent dye labeled MSCs (arrows).

Biochemical studies

Blood samples from all rats' tail veins were taken in heparinized capillary tubes just before the time for scarification to measure:

Serum Creatine Kinase muscle/Brain (CK-MB) & serum lactate dehydrogenase (LDH) enzyme levels to determine myocardial injury: Fresh serum's CK-MB activity was measured using a widely available CK-MB assay kit (Spinreact Co., Sant Esteve de Bas, Spain). A kit for assaying LDH was used to quantify it (Beyotime, Shanghai, China). As directed by the manufacturer, serum was incubated with an LDH working reagent to detect LDH levels (Thomas, 1998).

Also Cardiac tissue malondialdehyde (MDA) level (indirect index for lipid peroxidation): was calculated using the procedure outlined by Ruiz-Larnea et al. (1994). The level of cardiac MDA is expressed as (nmol/g tissue).

Histological Light microscopic studies

The hearts of the sacrificed animals were immediately removed, preserved in 10% formalin, and handled into paraffin blocks. Sections of the left ventricle were cut 5µm thick, and stained with:

a) Hematoxylin and eosin (Suvarna et al., 2018).

b) Masson's trichrome stain to detect collagen fibers (Suvarna et al., 2018).

c) Immunohistochemical staining of alpha-smooth muscle actin (α-SMA) and B-cell lymphoma 2 (Bcl-2): 5 µm heart sections were deparaffinized and rehydrated. Treatment with hydrogen peroxide 3% inhibited general natural peroxidase activity. Sections were then heated in citrate buffer (0.01 M, pH 6.0) in a water bath at 95°C for 30 minutes to extract antigens. A mouse anti-Bcl-2 antibody (1:100; Abcam, Cambridge, MA, USA) and an anti-alpha-smooth muscle actin (α-SMA) antibody (Abcam, ab5694, 1:100) were incubated on sections at 4°C for an overnight period. After that, the sample was incubated for 30 minutes at room temperature with a biotinylated anti-mouse secondary antibody (1:200; catalog no. ZDR-5307; Beijing Zhongshan Jinqiao Biotechnology Co., Ltd., Beijing, China). A colorimetric reaction was started when DAB was added. The slices were counterstained with Hx, and mounted with DPX. Positive expressions were represented by a brown reaction (Suchal et al., 2017).

Histological electron microscopic study

Cardiac muscle samples were cut into small pieces (0.5-1.0 mm^3), fixed for 2 h at 4 ◦C with 2.5% glutaraldehyde in a 0.1 M phosphate buffer (pH 7.4), and then post-fixed for 1.5 h at 4 ◦C with 1% osmium tetroxide. The sample was then dehydrated using acetone for 30 minutes and serially diluted with ethanol for 30 minutes. Lastly, the fixed specimens were implanted using epoxy resin (Epoxy Embedding Medium Kit; Sigma) (Suvarna et al., 2018). Semi- and ultra-thin sections were cut on an ultramicrotome (RMC PT-XL PowerTome Ultramicrotome).

Using an Olympus BX61 light microscope, semi-thin (1µm-850 nm) sections were stained with 1% toluidine blue and inspected. Ultra-thin slices were cut at a thickness of 70-90 nm, and they were subsequently stained with lead citrate as the counterstain and 2.5% uranyl acetate as the

primary stain. Eventually, the electron microscopy unit at the Faculty of Science, Alexandria University, Egypt, examined ultrathin sections using a JEM-1400 Plus (JEOL, Japan) transmission electron microscope (Dykstra and Reuss, 2003).

Morphometrical studies.

To ascertain the following, ten non-overlapping fields from various areas of each group were used:

- Mean area of collagen fibers (x200).
- Positive area of α-SMA and Bcl-2 immuno-positive cells (x200).

At the Anatomy and Embryology Department, Faculty of Medicine, Benha University, measurements were made using Leica Qwin-500 LTD software image analysis computer system Ltd. (Cambridge, UK).

Statistical studies.

The results were analyzed using SPSS 19.0 and formulated as the mean ± SD. ANOVA was employed to ascertain the statistical significance, followed by Tukey's multiple comparison tests. $P \leq 0.05$ was deemed significant.

Results

All examined parameters between subgroups of Group I (Control group) revealed no significant difference. So, Subgroup Ia was referred to them.

***Biochemical results*:**

Regarding the mean serum levels of CK-MB and LDH, there was a highly significant increase in CP and the withdrawal groups as compared to the control group ($P < 0.001$). The withdrawal group had a non-significant decrease in comparison to the CP group ($P = 0.97$ for CK-MB, $P = 0.95$ for LDH). While the CP plus Mangiferin and CP plus BM-MSCs groups demonstrated a significant decrease compared to the CP group ($P = 0.03$ and $P = 0.02$, respectively, for CM-MB and $P = 0.04$ and $P = 0.01$, respectively, for LDH), the CP plus Mangiferin and BM-MSCs group illustrated a highly significant decrease when compared to the CP group ($P < 0.001$). However, the CP plus Mangiferin and BM-MSCs group revealed an insignificant increase when compared to the control group ($P = 0.99$) (Table 1).

Regarding the mean tissue level of MDA, there was a highly significant increase in the CP and withdrawal groups as compared to the control group ($P < 0.001$). The withdrawal group had a non-significant decrease in comparison to the CP group ($P = 0.1$). While the CP plus Mangiferin and the CP plus BM-MSCs groups demonstrated a significant decrease compared to the CP group ($P = 0.02$ and $P = 0.01$, respectively), the CP plus Mangiferin and BM-MSCs group illustrated a highly significant decrease when compared to the CP group ($P < 0.001$). However, the CP plus Mangiferin and BM-MSCs group revealed an insignificant increase when compared to the control group ($P = 0.92$) (Table 1).

Table (1): Serum levels of CK-MB, LDH, and tissue level of MDA among the studied groups

	Group I (Control group)	Group II (CP group)	Group III (Withdrawal group)	Group IV (CP plus Mangiferin group)	Group V (CP plus BM-MSCs group)	Group VI (CP plus Mangiferin and BM-MSCs group)	P value
CK-MB Mean ±SD **U/L**	**132.98 ± 1.07**	**440.25± 7.4**	**410.6±5.6**	**293.7± 8.6**	**282.2± 9.7**	**146.8 ± 1.4**	**<0.001[a] < 0.001[b] 0.97[c] 0.03[d] 0.02[e] < 0.001[f] 0.99[g]**
LDH Mean ±SD **U/L**	**169.33 ± 1.07**	**406.05 ± 7.4**	**377.3±5.6**	**288.4 ± 5.3**	**264.33± 2.4**	**172.03 ± 1.4**	**< 0.001[a] < 0.001[b] 0.95[c] 0.04[d] 0.01[e] < 0.001[f] 0.99[g]**
MDA Mean ±SD **Nmol/g tissue**	**7.2 ± 0.3**	**16.5 ± 1.4**	**14.9 ±0.15**	**14.2± 0.61**	**13.26 ± 0.38**	**7.7± 0.57**	**< 0.001[a] < 0.001[b] 0.1[c] 0.02[d] 0.01[e] < 0.001[f] 0.92[g]**

Number of samples (10 in each group), CK-MB: Creatine Kinase muscle/Brain, LDH: Lactate dehydrogenase, MDA: malondialdehyde, Values are presented as mean ± SD.

a Comparison between the control group and the CP group
b Comparison between the control group and the Withdrawal group.
c Comparison between the CP group and the Withdrawal group.
d Comparison between CP group and CP plus Mangiferin group.
e Comparison between CP group and CP plus BM-MSCs group.
f Comparison between CP group and CP plus Mangiferin and BM-MSCs group.
g Comparison between the control group and CP plus Mangiferin and BM-MSCs group.

Histological light microscopic, morphometrical and statistical results

Hematoxylin and eosin stain

Sections of the control group stained with H&E exhibited regularly arranged branching and anastomosing cardiac muscle fibers with centrally located vesicular nuclei and acidophilic sarcoplasm. Muscle fibers were separated by blood capillaries and connective tissue cells (Figures 2A and 3A).

However, H&E-stained sections of the CP group displayed degenerated muscle fibers with vacuolated sarcoplasm. Some muscle fibers appeared with perinuclear cytoplasmic depletion (myolysis) and dilated congested blood vessels with extravasated RBCs. Also, leukocytic infiltration, deeply stained shrunken pyknotic nuclei, and fibrosis were noticed (Figures 2B and 3B).

Also, the withdrawal group H&E-stained sections revealed separated degenerated cardiac muscle fibers with fragmented cardiac muscle fibers. Congested dilated blood vessels, leukocytic inflammatory infiltrate, deeply stained shrunken pyknotic fiber nuclei, and fibrosis were also observed. There was hypertrophy of cardiac muscle fibers (Figures 2C and 3C).

Sections of the CP plus Mangiferin group stained with H&E exhibited features nearly similar to those of the control group. While some muscle fibers with vacuolated sarcoplasm were separated by slightly dilated but not congested blood capillaries, a few pyknotic nuclei were also observed (Figures 2D and 3D).

CP plus BM-MSCs group H&E sections displayed features nearly similar to the control group. But there was separation of some fiber's bundles. Occasional pyknotic nuclei were also observed (Figures 2E and 3E).

Moreover, H&E-stained sections of the CP plus Mangiferin and BM-MSCs group demonstrated features similar to those of the control group, with a slight separation of cardiac muscle fibers. But occasional pyknotic nuclei were also observed (Figures 2F and 3F).

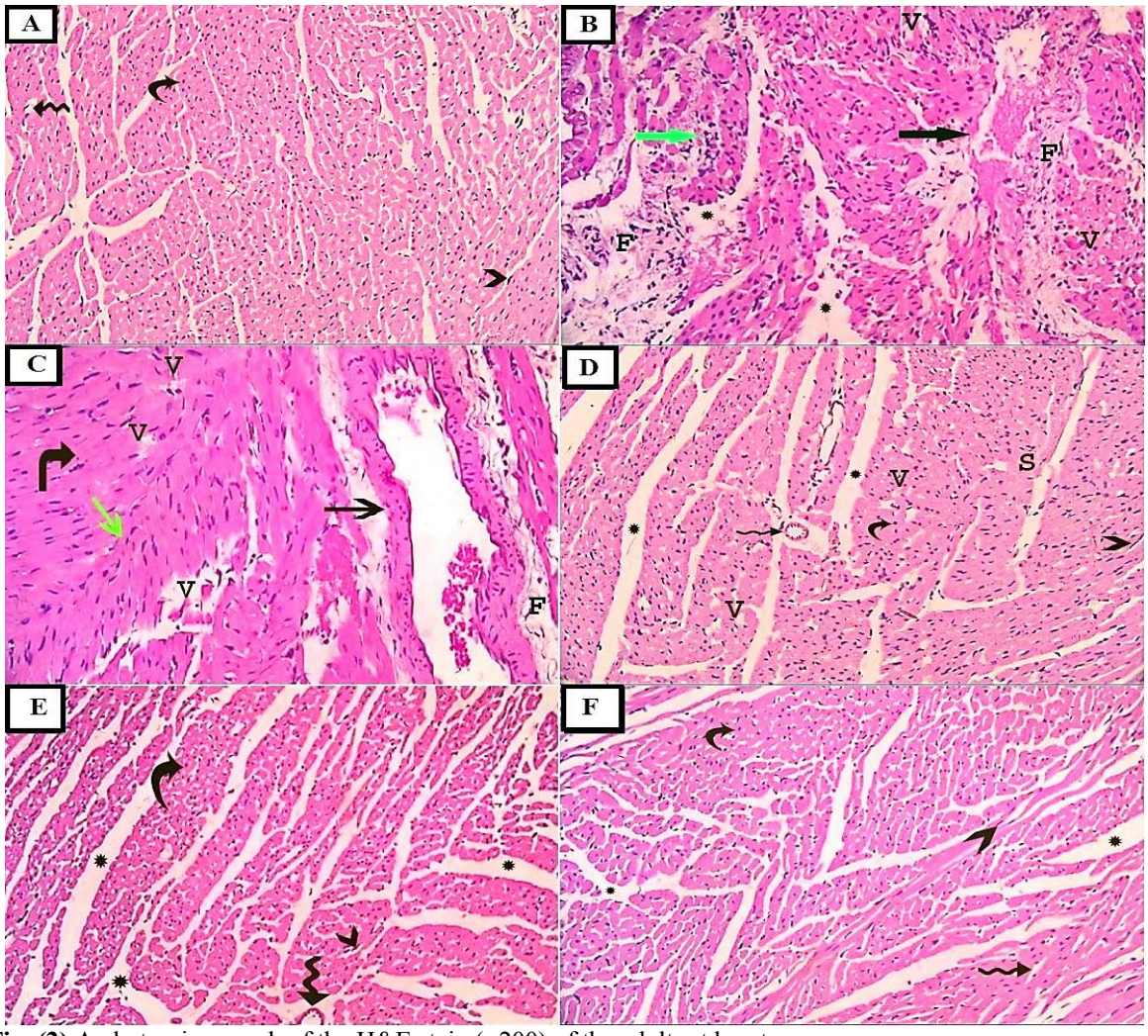

Fig. (2) A photomicrograph of the H&E stain (×200) of the adult rat heart

(A) Group I (control group) shows well-organized cardiac muscle fibers that exhibit acidophilic sarcoplasm and centrally located vesicular nuclei (curved arrow). N0rmal blo0d capillaries (zigzag arrow) and dark nuclei of fibr0blasts (arr0w heads) are seen between the cardiac muscle fibers.

(B) Group II (CP group) reveals separated cardiac muscle fibers (asterisks). Many fibers appeared degenerated with vacuolated sarcoplasm (V). Congested blood vessels, extravasated red blood cells (black arrow), leukocytic inflammatory infiltrate (green arrow), and fibrosis (F) were also observed.

(C) Group III (withdrawal group) illustrates separated cardiac muscle fibers; many fibers appeared degenerated with fragmented cardiac muscle fibers (V). Congested dilated blood vessels (black arrow), leukocytic inflammatory infiltrate (green arrow), and perivascular fibrosis (F) were also observed, and there is hypertrophy of cardiac fibers (right-angle arrow).

(D) Group IV (CP plus Mangiferin group) demonstrating separated cardiac muscle fibers (asterisks) with acidophilic sarcoplasm (S) and centrally located vesicular nuclei (curved arrow). Some fibers still have vacuolated sarcoplasm (V). Dilated but not congested blood capillaries (zigzag arrow) and dark nuclei of fibroblasts (arrowhead) are seen between the cardiac muscle fibers.

(E) Group V (CP plus BM-MSCs group) showing slightly separated cardiac muscle fibers (asterisks) with acidophilic sarcoplasm and centrally located vesicular nuclei (curved arrow). Normal blood capillaries (zigzag arrow) and dark nuclei of fibroblasts (arrowhead) are seen between the cardiac muscle fibers.

(F) Group VI (CP plus Mangiferin and BM-MSCs group) illustrating slightly separated cardiac muscle fibers (asterisks) with acidophilic sarcoplasm and centrally located vesicular nuclei (curved arrow). Normal blood capillaries (zigzag arrow) and dark nuclei of fibroblasts (arrowhead) are seen between the cardiac muscle fibers.

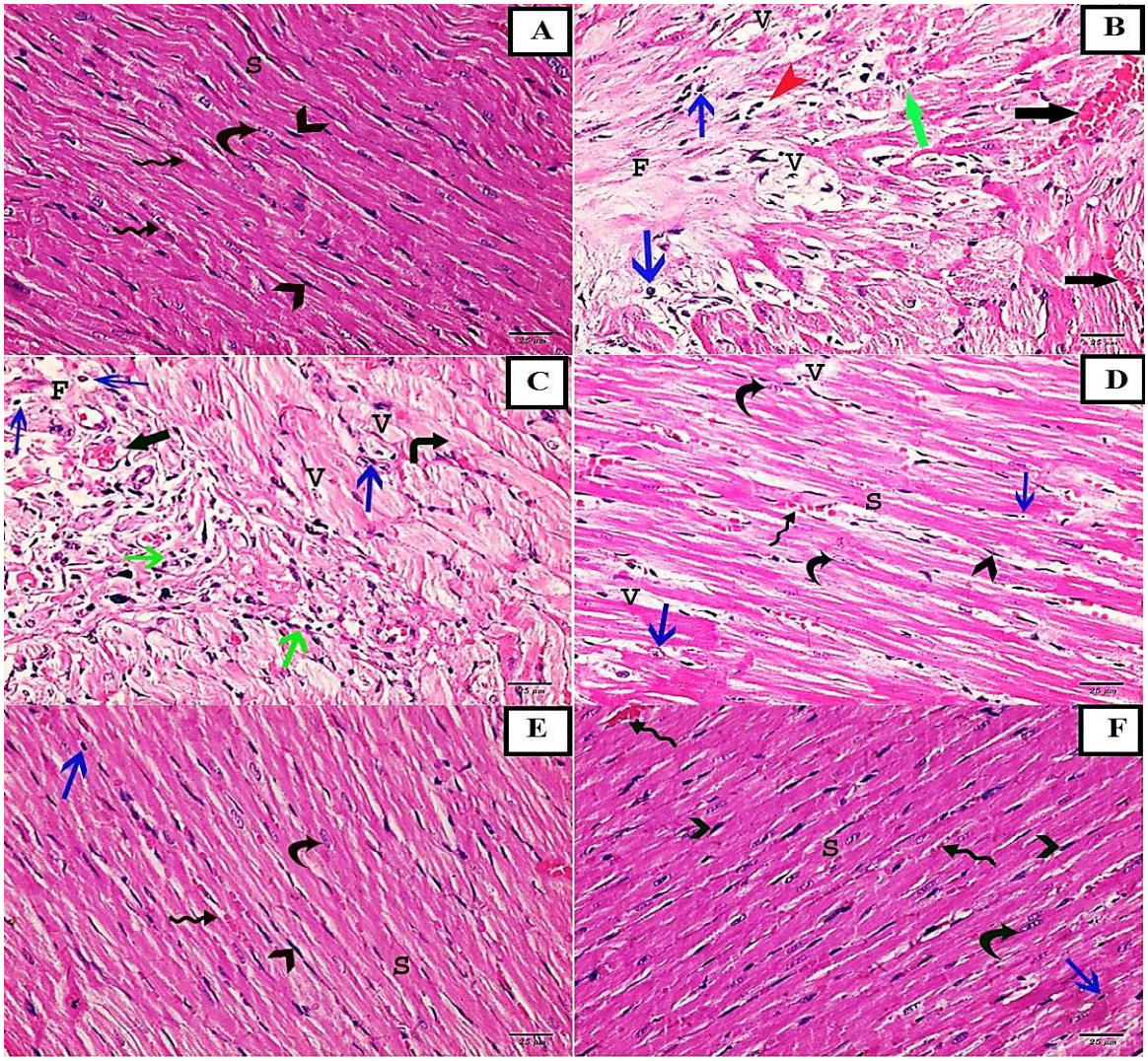

Fig. (3) A photomicrograph of the H&E stain (×400) of the adult rat heart;

(A) Group I (control group) shows regularly arranged branching and anastomosing cardiac muscle fibers with centrally located vesicular nuclei (curved arrow) and acidophilic sarcoplasm (S), separated by blood capillaries (zigzag arrow) and connective tissue cells dark nuclei (fibroblasts) (arrowhead) between muscle fibers.

(B) Group II (CP group) myocardium illustrating vacuolated sarcoplasm (V) Some muscle fibers exhibit perinuclear cytoplasmic depletion (myolysis) (red arrowhead). Dilated congested blood vessels with extravasated red blood cells (black arrow), leukocytic infiltration (green arrow), deeply stained shrunken pyknotic nuclei (blue arrow), and fibrosis (F) were noticed.

(C) Group III (withdrawal group) reveals separated cardiac muscle fibers. Perinuclear cytoplasmic depletion (myolysis) or vacuolation (V), congested capillary (black arrow), leukocytic inflammatory infiltrate (green arrow), deeply stained shrunken pyknotic nuclei (blue arrow), and fibrosis (F) were also observed. There is hypertrophy of cardiac fibers (right-angle arrow).

(D) Group IV (CP plus Mangiferin group) showing separated branching and anastomosing cardiac muscle fibers with centrally located vesicular nuclei (curved arrow) and acidophilic sarcoplasm (S), separated by slightly congested blood capillaries (zigzag arrow) and connective tissue cells dark nuclei (fibroblasts) (arrowhead) between muscle fibers, but still, there is some vacuolation of sarcoplasm (V); a few pyknotic nuclei were also observed (blue arrow).

(E) Gr0up V (CP plus BM-MSCs group) viewing slightly separated branching and anastomosing cardiac muscle fibers with centrally located vesicular nuclei (curved arrow) and acidophilic sarcoplasm (S), separated by slightly congested blood capillaries (zigzag arrow) and connective tissue cells dark nuclei (fibroblasts) (arrowhead) between muscle fibers; occasional pyknotic nuclei were also observed (blue arrow).

(F) Group VI (CP plus Mangiferin and BM-MSCs group) displaying regularly arranged branching and anastomosing cardiac muscle fibers with centrally located vesicular nuclei (curved arrow) and acidophilic sarcoplasm (S), separated by blood capillaries (zigzag arrow) and connective tissue cells dark nuclei (fibroblasts) (arrowhead) between muscle fibers; occasional pyknotic nuclei were also observed (blue arrow).

Masson's trichrome stain:

Masson's stained sections of the control group showed a very minimal amount of collagen fibers in between muscle fibers (Figure 4A). However, CP group Masson's stained sections demonstrated an increased amount of collagen fibers in between muscle fibers and around blood vessels (Figure 4B).

Also, the withdrawal group's stained sections showed an increased amount of collagen fibers in between muscle fibers and around blood vessels (Figure 4C). Whereas, Masson's stained sections of the CP plus Mangiferin group illustrated a moderate amount of collagen fibers in-between muscle fibers and around blood vessels (Figure 4D).

CP plus the BM-MSCs group Masson's stained sections showed a minimal amount of collagen fibers in between muscle fibers and around blood vessels (Figure 4E). Masson's stained section of the CP plus Mangiferin and BM-MSCs group revealed a very minimal amount of collagen fibers in between muscle fibers (Figure 4F).

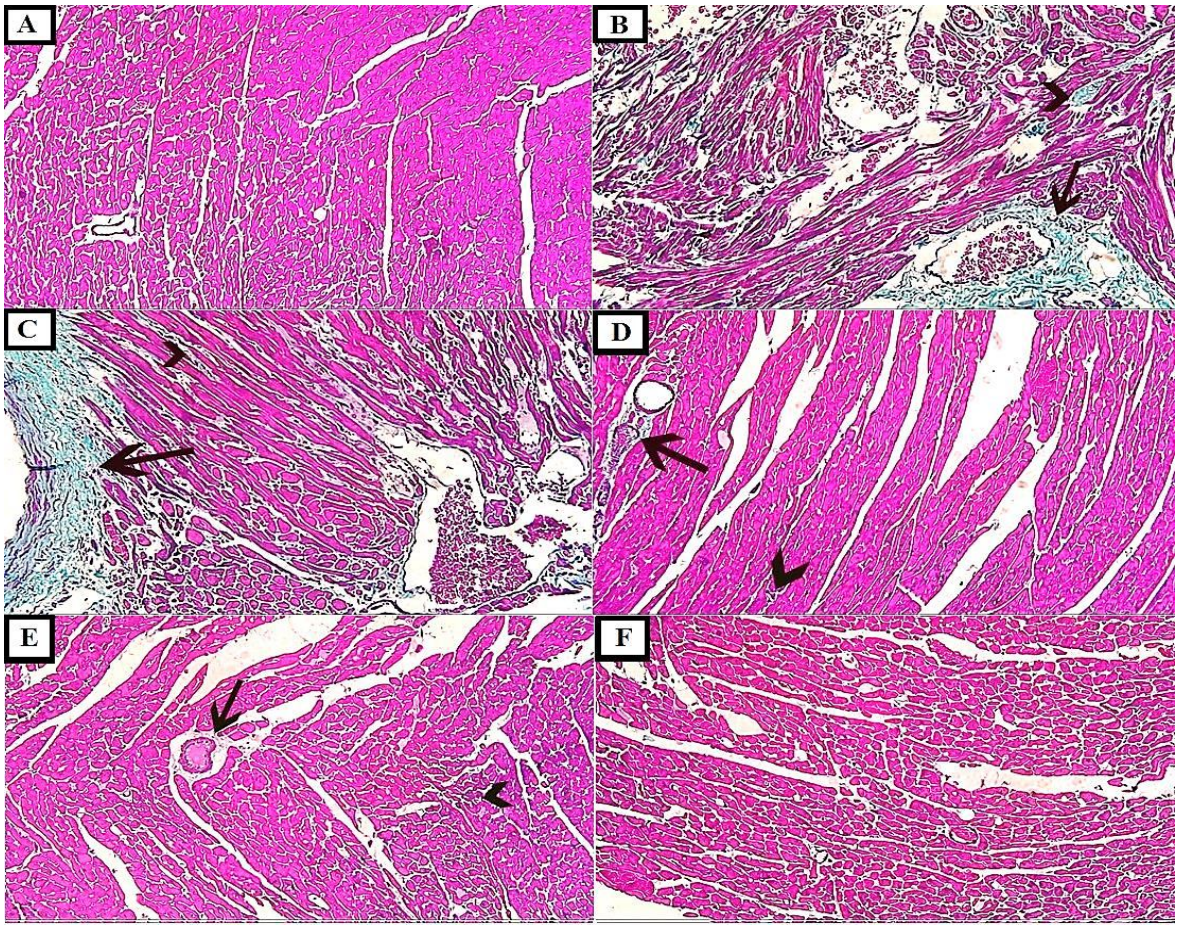

Fig. (4) A photomicrograph of Masson's Trichrome stain (×200) of the adult rat cardiac muscle;
(A) Group I (Control group) shows very minimal amount of collagen fibers in between the muscle fibers.
(B) Group II (CP group) reveals increased amount of collagen fibers in-between the muscle fibers (arrow head) and around blood vessels (black arrow).
(C) Group III (Withdrawal group) shows increased amount of collagen fibers in-between the muscle fibers (arrowhead) and around blood vessels (black arrow).
(D) Group IV (CP plus Mangiferin group) demonstrated a moderate amount of collagen fibers in between the muscle fibers (arrowhead) and surrounding blood vessels (black arrow).
(E) Group V (CP plus BM-MSCs group) shows a minimal amount of collagen fibers in between the muscle fibers (arrowhead) and around blood vessels (black arrow).
(F) Group VI (CP plus Mangiferin and BM-MSCs group) illustrates a very minimal amount of collagen fibers in between the muscle fibers.

Concerning the morphological results of the mean area % of collagen fiber deposition, there was a highly significant increase in the CP and withdrawal groups compared to the control group (P<0.001). The withdrawal group had a non-significant decrease in comparison to the CP group (P = 0.9). While the CP plus Mangiferin and CP plus BM-MSCs groups demonstrated a significant decline in comparison to the CP group (P = 0.04), the CP plus Mangiferin and BM-MSCs group showed a highly significant decrease when compared to the CP group (P<0.001) and displayed a non-significant increase when compared to the control group (P = 0.99) (Table 2, Figure 5).

Table (2): Comparison between area percentages of collagen fiber deposition among the studied groups.

	Group I (Control group)	**Group II (CP group)**	**Group III (Withdrawal group)**	**Group IV (CP plus Mangiferin group)**	**Group V (CP plus BM-MSCs group)**	**Group VI (CP plus Mangiferin and BM-MSCs group)**	**P value**
Area % of collagen fiber deposition mean ± SD	1.7 ± 0.55	29. 2 ± 7.9	28.07 ± 4	19.9 ± 0.66	18.49 ± 1.27	3.59 ± 1.2	**< 0.001[a]** **< 0.001[b]** **0.9 [c]** **0.04[d]** **0.04[e]** **< 0.001[f]** **0.99[g]**

Number of samples (10 in each group), Values are presented as mean ± SD.

a Comparison between the control group and the CP group

b Comparison between the control group and the Withdrawal group.

c Comparison between the CP group and Withdrawal group.

d Comparison between CP group and CP plus Mangiferin group.

e Comparison between CP group and CP plus BM-MSCs group.

f Comparison between CP group and CP plus Mangiferin and BM-MSCs group.

g Comparison between the control group and CP plus Mangiferin and BM-MSCs group.

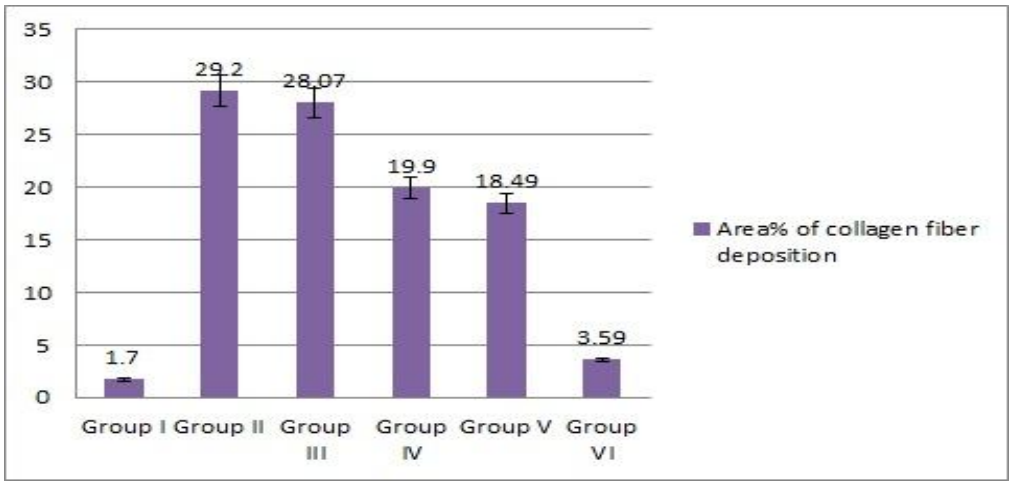

Fig. (5). A histogram illustrating a highly significant increase in groups II and III mean area % of collagen fibers deposition as compared to the control group. Group III has a non-significant decrease in comparison to group II. While groups IV & and V demonstrated a significant decrease compared to group II. Group VI showed a highly significant diminution when compared to Group II and an insignificant rise when compared to the control group.

Immunohistochemistry:

α-SMA stained sections of the cardiac muscle of the control group showed very minimal expression mainly in the wall of the blood vessels (Figure 6A). However, CP and Withdrawal groups; α-SMA stained cardiac muscle sections demonstrated increased brown coloration of sarcoplasm and in the capillary wall that indicated strong positive cytoplasmic expression (Figures 6B & 6C). Whereas α-SMA stained sections of cardiac muscle of CP plus Mangiferin group showed moderate αSMA expression (Figure 6D), and that of CP plus BM-MSCs group showed minimal α-SMA expression (Figure 6E). While CP plus Mangiferin and BM-MSCs group cardiac muscle sections showed very minimal α-SMA expression mainly in the wall of the blood vessels (Figure 6F).

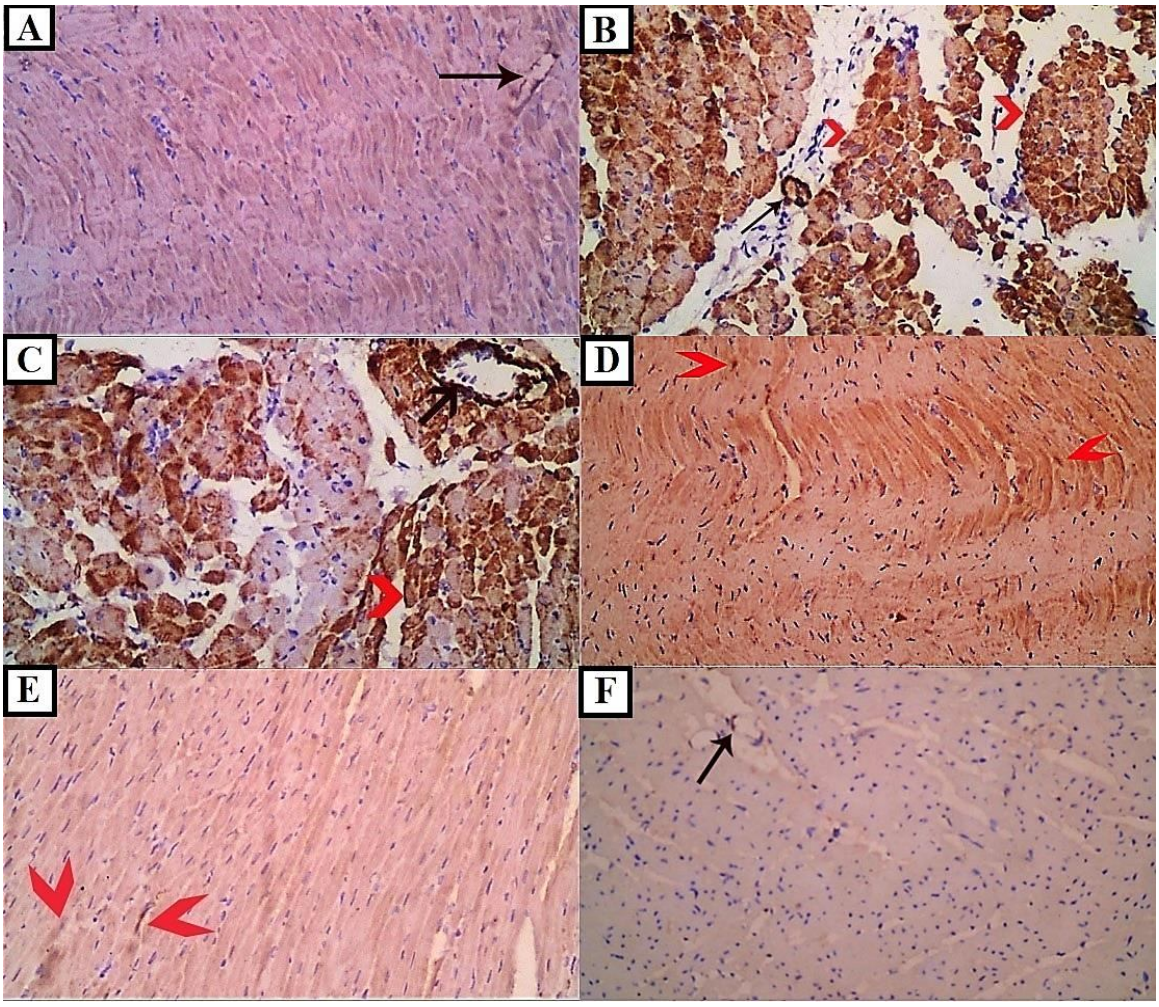

Fig. (6). α-SMA immunostained (×200) photomicrograph of the rat cardiac muscle

(A) Group I (the control group) demonstrated very minimal α-SMA expression, mainly in the wall of the blood vessels (black arrow).

(B) Group II (CP group) showing increased brown coloration of sarcoplasm (red arrowhead) and in the capillary wall (black arrow) that indicates strong positive diffuse cytoplasmic α-SMA expression.

(C) Group III (withdrawal group) revealed increased brown coloration of sarcoplasm (red arrowhead) and in the capillary wall (black arrow), which indicates a strong positive cytoplasmic α-SMA reaction.

(D) Group IV (CP plus Mangiferin group) showing moderate α-SMA expression (red arrowheads)

(E) Group V (CP plus BM-MSCs group) illustrating minimal α-SMA expression (red arrowheads)

(F) Group VI (CP plus Mangiferin and BM-MSCs group) shows very minimal α-SMA expression mainly in the wall of the blood vessels (black arrow).

Concerning the % positive area of α-SMA immunoreactivity, the CP and withdrawal groups illustrated a highly significant rise compared to the control group (P<0.001). The withdrawal group had a non-significant decrease in comparison to the CP group (P = 0.97). While the CP plus Mangiferin and CP plus BM-MSCs groups showed a significant decrease in comparison to the CP group (P = 0.04 and P = 0.02, respectively), Moreover, the CP plus Mangiferin and BM-MSCs group demonstrated a highly significant decrease when compared to the CP group (P<0.001) and displayed a non-significant rise when compared to the control group (P = 0.98) (Table 3 and Figure 8).

Bcl-2-stained sections of the cardiac muscle of the control group showed increased brown coloration of sarcoplasm, indicating a strong positive cytoplasmic reaction (Figure 7A). However, CP and withdrawal group Bcl-2-stained sections showed decreased brown coloration of sarcoplasm, indicating a very weak cytoplasmic reaction (Figures7B and 7C). CP plus Mangiferin group Bcl-2 stained sections showed increased brown coloration of sarcoplasm that indicated a positive cytoplasmic reaction (Figure 7D). Moreover, Bcl-2-stained sections of the CP plus BM-MSCs group showed increased brown coloration of sarcoplasm that indicated a strong positive cytoplasmic reaction (Figure 7E), and Bcl-2-stained sections of the cardiac muscle of the CP plus Mangiferin and BM-MSCs group showed increased brown coloration of sarcoplasm that indicated a strong positive cytoplasmic reaction (Figure 7F).

Regarding the % positive area of Bcl-2 immunoreactivity in the CP and withdrawal groups, it illustrated a highly significant decrease compared to the control group (P<0.001). The withdrawal group had a non-significant increase in comparison to the CP group (P = 0.89). While the CP plus Mangiferin and CP plus BM-MSCs groups showed significant increases in comparison to the CP group (P = 0.04 and P = 0.02, respectively), Moreover, the CP plus Mangiferin and BM-MSCs group demonstrated a highly significant increase when compared to the CP group (P<0.001) and displayed a non-significant decline when compared to the control group (P = 0.98) (Table 3 and Figure 8).

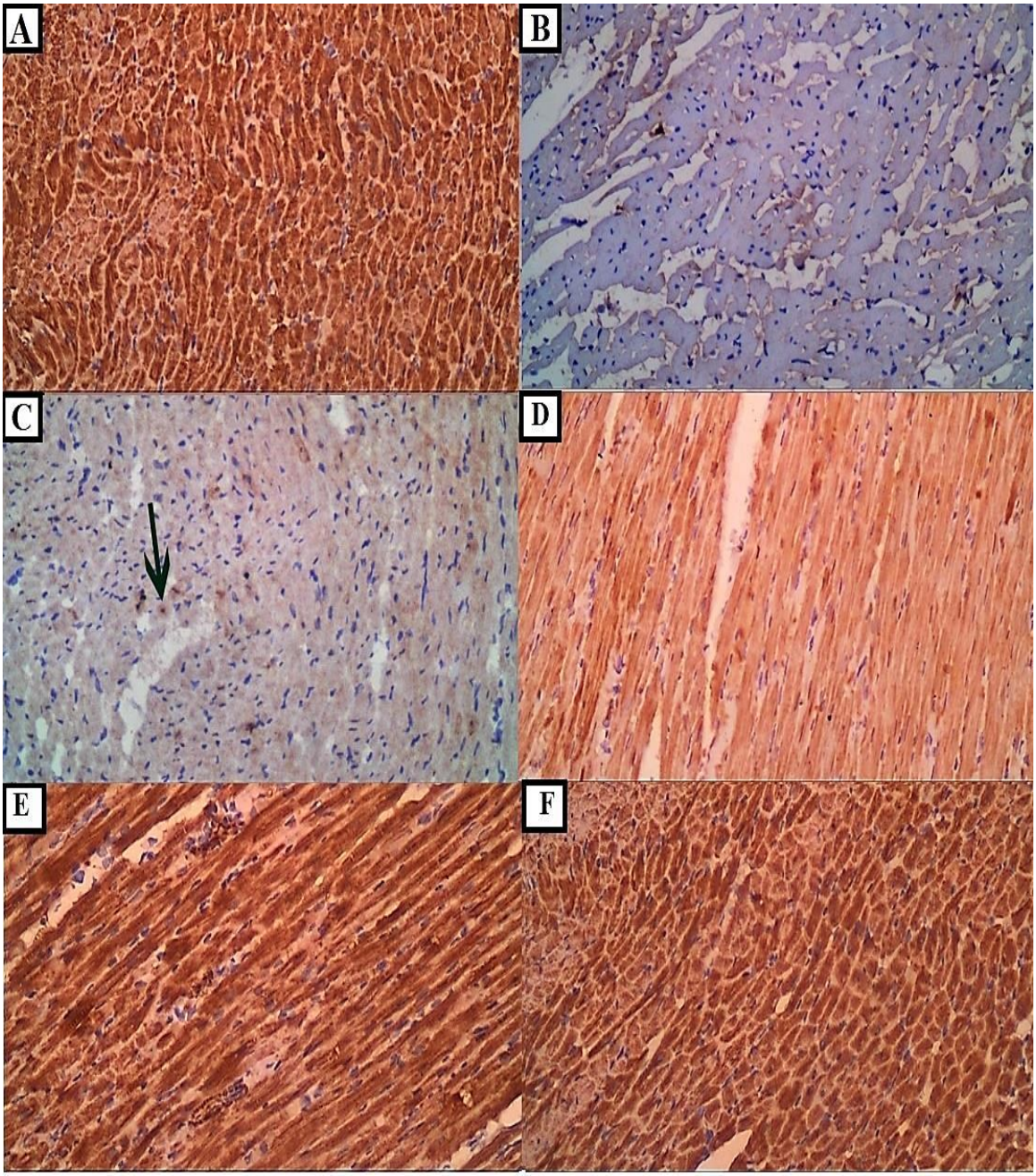

Fig. (7). Bcl-2 immunostained (×200) photomicrograph of cardiac muscle

(A) Group I (control group) illustrates increased brown coloration of sarcoplasm, which indicates a strong positive cytoplasmic Bcl-2 reaction.

(B) Group II (CP group) shows decreased brown coloration of sarcoplasm, which indicates a very weak cytoplasmic Bcl-2 reaction.

(C) Group III (withdrawal group) reveals decreased brown coloration of sarcoplasm, which indicates a weak cytoplasmic Bcl-2 reaction (arrow).

(D) Group IV (CP plus Mangiferin group) shows increased brown coloration of sarcoplasm, which indicates a positive cytoplasmic Bcl-2 reaction.

(E) Group V (CP plus BM-MSCs group) reveals increased brown coloration of sarcoplasm, which indicates a strong positive cytoplasmic Bcl-2 reaction.

(F) Group VI (CP plus Mangiferin and BM-MSCs group) demonstrates increased brown coloration of sarcoplasm, which indicates a strong positive cytoplasmic Bcl-2 reaction.

Table (3): Immunohistochemical markers among the studied groups.

	Group I (Control group)	Group II (CP group)	Group III (Withdrawal group)	Group IV (CP plus Mangiferin group)	Group V (CP plus BM-MSCs group)	Group VI (CP plus Mangiferin and BM-MSCs group)	P value
α-SMA **mean ±SD**	1.93 ±0.54	41.02± 1.3	39.2± 4.4	32.69± 0.56	28.89 ±5.04	3.59 ± 1.2	**< 0.001[a]** **< 0.001[b]** **0.97[c]** **0.04[d]** **0.02[e]** **< 0.001[f]** **0.98[g]**
Bcl-2 **mean ±SD**	31.79± 5.4	10.18 ±0.34	13.3 ± 4.3	20.03 ±0.66	21.49 ± 0.61	29.8 ± 5.5	**< 0.001[a]** **< 0.001[b]** **0.89[c]** **0.04[d]** **0.02[e]** **< 0.001[f]** **0.98[g]**

Number of samples (10 in each group).
α-SMA: alpha-smooth muscle actin, **Bcl-2:** B-Cell Lymphoma Values are presented as mean±SD.
a Comparison between the control group and the CP group
b Comparison between the control group and the Withdrawal group.
c Comparison between the CP group and the Withdrawal group.
d Comparison between CP group and CP plus Mangiferin group.
e Comparison between CP group and CP plus BM-MSCs group.
f Comparison between CP group and CP plus Mangiferin and BM-MSCs group.
g Comparison between the control group and CP plus Mangiferin and BM-MSCs group.

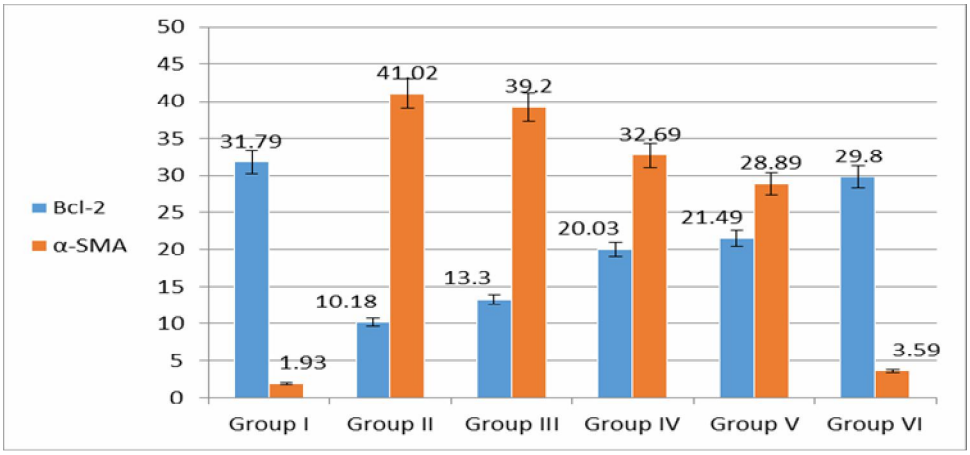

Fig. (8). A histogram demonstrating a highly significant reduction in groups II and III mean areas of Bcl-2 immunoreactivity compared to the control group Group III has a non-significant increase in comparison to Group II. While groups IV and V demonstrated a significant rise compared to group II, group VI showed a highly significant rise when compared to group II and an insignificant decline when compared to the control group. However, it demonstrated a highly significant rise in groups II and III mean areas of α-SMA immunoreactivity compared to the control group. Group III has a non-significant reduction in comparison to Group II. While groups IV and V demonstrated a significant decrease compared to group II, group VI showed a highly significant reduction when compared to group II and an insignificant rise when compared to the control group.

Histological electron microscopy results

Ultrathin sections of the control group illustrated cardiomyocytes with a centrally located euchromatic nucleus, many perinuclear mitochondria with prominent cristae, and elongated mitochondria that appeared between myofibrils. Additionally, sarcomeres with a central dark A-band and two light hemi-I-bands were discovered in the periphery. These sarcomeres were bordered on each side by a Z-line. The M-line splits the pale H-zone in the middle of the A-band. Additionally, two cardiomyocytes were separated by a regular intercalated disc that displayed Fasciae adherents were usually located in the transverse portions of the disc. Desmosomes were found primarily in the transverse portions of the disc. Gap junctions were usually restricted to longitudinal portions of the disc (Figures 9A &B).

CP group ultrathin sections showed sarcomere with thick interrupted Z-line with dilated T tubule. Sarcoplasm showed rarefaction. Small condensed clumps of chromatin that created chromatin balls could be found in the indented, apoptotic nucleus of cardiomyocytes with perinuclear chromatolysis and small-sized degenerated mitochondria. Disruption and loss of myofibrils and swollen mitochondria were noticed. The intercalated disc appeared interrupted (Figures 9C and D).

Ultrathin images of the withdrawal group showed a nucleus with wide areas of chromatin loss and areas of rarefaction. Most of the mitochondria illustrated disrupted vacuolated cristae. Disruption and loss of myofibrils with thick interrupted Z-lines and dilated T tubules were noticed. The intercalated disc appeared interrupted (Figures 9E and F).

CP plus Mangiferin group ultrathin images revealed a nearly normal structure of cardiac myocytes with a normal arrangement of myofibrils. However, there were some degenerated myofibrils with mildly dilated T tubules and mild nuclear irregularity. Nearly normal mitochondria, but some degenerated mitochondria were noticed in the presence of lysosomes. Additionally, two cardiomyocytes are separated by a regular intercalated disc (Figures 10A and B).

The CP plus BM-MSCs group ultrathin sections showed cardiomyocytes nearly similar to the control. The presence of lysosomes and the rarefaction of sarcoplasm were noticed. Two cardiomyocytes were separated by a regular intercalated disc. Dilatation of the sarcoplasmic reticulum and separation of myofibrils were observed (Figures 10C and D).

Ultrathin sections of the CP plus Mangiferin and BM-MSCs group demonstrated cardiomyocytes similar to the control group. Two cardiomyocytes were separated by a regular intercalated disc (Figures 10E and F)

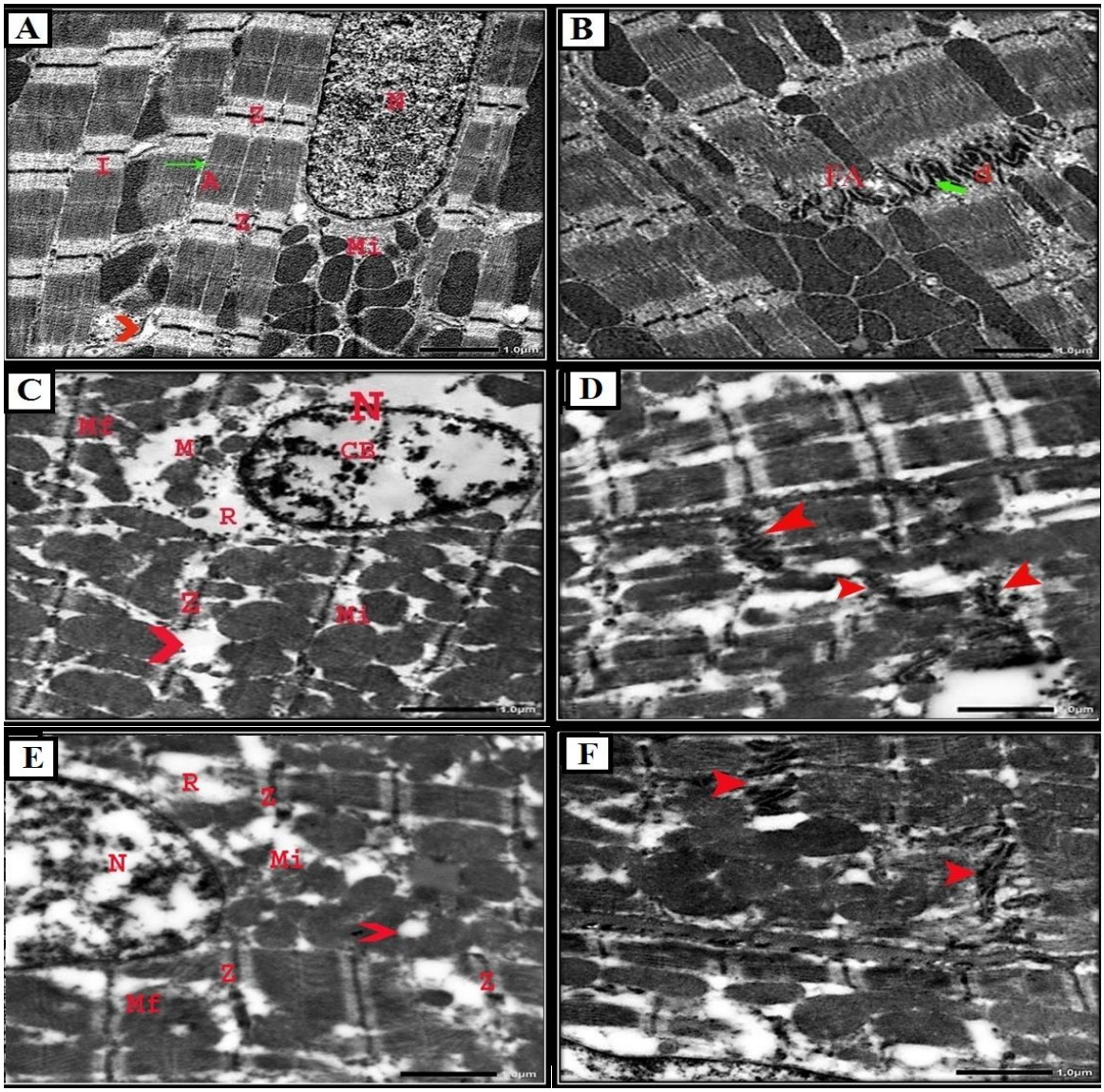

Fig. (9). Electron micrograph (×5000) of the rat myocardium of

(A) Group I (control group) demonstrates a cardiomyocyte with a centrally located euchromatic nucleus (N), many perinuclear mitochondria (Mi) with prominent cristae, and elongated mitochondria appear between myofibrils. Sarc0meres that were bound on each side by a Z-line (Z) with a central dark A-band (A) and two light hemi I-bands (I) in the periphery A Pale H-zone could be seen in the center of the A-band, bisected by the M-line (green arrow) and the T tubule (red arrowhead).

(B) Group I (control group) shows two cardiomyocytes separated by a regular intercalated disc, showing fascia adherens (FA) and desmosomes (d) are seen in the transverse parts of the disc, whereas gap junctions (green arrow) are in the longitudinal part.

(C) Group II (CP group) showing sarcomere with thick interrupted Z line (Z) with dilated T tubule (red arrowhead apoptotic). Sarcoplasm shows rarefaction (R). The apoptotic indented nucleus of cardiomyocyte (N) contains small condensed clumps of chromatin forming chromatin balls (CB) with perinuclear chromatolysis and small-sized degenerated mitochondria (M). Notice the disruption and loss of myofibrils (Mf) and swollen mitochondria (Mi).

(D) Group II (CP group) reveals two cardiomyocytes separated by an interrupted intercalated disc (red arrowhead).

(E) Group III (withdrawal group) showing nucleus (N) with wide areas of chromatin loss and areas with rarefaction (R). Most mitochondria show disrupted vacuolated cristae (Mi). Notice the disruption and loss of myofibrils (Mf) with a thick interrupted Z line (Z) and dilated T tubule (red arrowhead).

(F) Group III (withdrawal group) illustrates two cardiomyocytes separated by a slightly interrupted intercalated disc (red arrowhead).

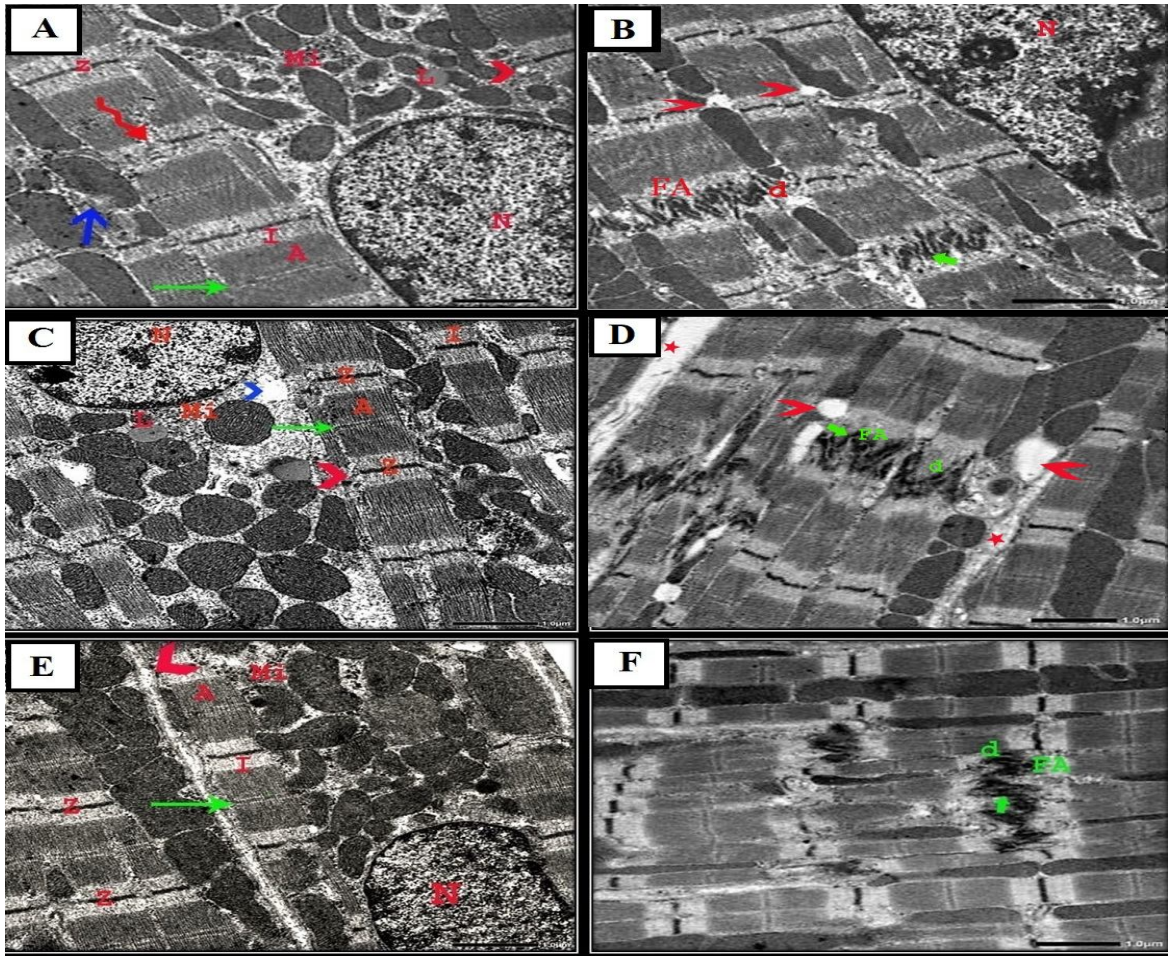

Fig. (10). Electron micrograph (×5000) of the rat myocardium of

(A) Group IV (CP plus Mangiferin group) reveals the near-normal structure of cardiac myocytes with a normal arrangement of myofibrils and sarcomeres with a central dark A-band (A), two pale hemi I-bands (I), and a Z-line (Z) on each side. In the middle of the A-band, where the M-line (green arrow) splits it in half, a faint H-zone could be seen, but there are some degenerated myofibrils (zigzag red arrow) with a T tubule (red arrowhead) and a nucleus (N). Nearly normal mitochondria (Mi), but some degenerated mitochondria (blue arrow) were noticed. Notice the presence of the lysosome (L).

(B) Group IV (CP plus Mangiferin group) showing two cardiomyocytes separated by regular intercalated disc showing fascia adherens (FA) and desmosomes (d) are seen in transverse parts of the disc, whereas gap junctions (green arrow) are in the longitudinal part, mild nuclear irregularity (N), and mildly arrowhead dilated T tubule (red arrowhead) were noticed.

(C) Group V (CP plus BM-MSCs group) showed cardiomyocytes with a centrally located euchromatic nucleus (N), many perinuclear mitochondria (Mi) with prominent cristae, and mitochondria (Mi) with abundant cristae were distributed between myofibrils. Sarcomeres with a center dark A-band (A), two light hemi I-bands (I) in the periphery, and a Z-line (Z) encircling them on each side in the middle of the A-band, the M-line (green arrow) is cut through a light H-zone with a T tubule (red arrowhead). Notice the presence of the lysosome (L) and the rarefaction of the sarcoplasm (blue arrowhead).

(D) Group V (CP plus BM-MSCs group) illustrating two cardiomyocytes separated by a regular intercalated disc, showing fascia adherens (FA) and desmosomes (d) are seen in the transverse parts of the disc, whereas gap junctions (green arrow) are in the longitudinal part. Dilatation of the sarcoplasmic reticulum (red arrowhead) and separation of myofibrils (star) are observed.

(E) Group VI (CP plus Mangiferin and BM-MSCs group) shows cardiomyocytes with a centrally located euchromatic nucleus (N), many perinuclear mitochondria (Mi) with prominent cristae, and elongated mitochondria appearing between myofibrils. Sarcomeres with a center dark A-band (A), two light hemi I-bands (I), and a Z-line (Z) bounding them on each side The M-line (green arrow) splits the middle of the pale H-zone seen in the center of the A-band with the T tubule (red arrowhead).

(F) Group VI (CP plus Mangiferin and BM-MSCs group) demonstrating two cardiomyocytes separated by intact intercalated disc fascia adherens (FA) and desmosomes (d) are seen in transverse parts of the disc, whereas gap junctions (green arrow) are in the longitudinal part.

Discussion

A well-known immunosuppressive and anticancer drug is cyclophosphamide. Its toxicity now places restrictions on its wider clinical application. Cardiotoxicity is one of the clinical risks preventing cyclophosphamide from being used (Ayza et al., 2020).

The CK-MB and LDH are significant serum biomarkers of cardiac injury. Lactate dehydrogenase is the enzyme that catalyzes the interconversion of pyruvate and lactate in body tissues, particularly in cardiac muscles. The CK-MB, a biomarker of myocardial infarction, is released into the bloodstream following cardiac damage (Safdar et al., 2017).

In the existing study, CK-MB and LDH serum levels had a highly significant increase in the CP group compared to the control group. This was in line with Liu et al. (2015). This observation was elucidated by Shanmugarajan et al. (2008), who demonstrated that one of the several effects of CP is direct injury to the myocardium endothelium with the discharge of CK-MB and LDH enzymes into the bloodstream, defining the degree of myocardial tissue injury and resulting in myocardial cell death.

Moreover, the mean tissue level of MDA had a significant elevation in the CP group as compared to the control group. This is in coincidence with the MDA finding of Emeka et al. (2021).

The CP group histologically stained sections in the running study conformed to those of the CP rats group noticed in the Helal et al. (2020) study, which revealed atrophic, disordered, disorganized, and widely spaced-apart cardiac muscle fibers with pyknotic nuclei, vacuolated sarcoplasm, RBC extravasation between cardiomyocytes, and significant deposition of collagen fibers between cardiomyocytes. Extravasation of RBCs may have been due to blood vessel walls' weakness from inflammation, making them vulnerable to damage, vascular leakage, endothelial cell detachment, tissue edema, and interstitial bleeding (Zaghloul et al., 2020).

Present ultrathin sections of CP group illustrated sarcomere with thick interrupted Z-line with dilated T tubule, sarcoplasm shows rarefaction, the apoptotic indented nucleus of cardiomyocyte containing small condensed clumps of chromatin forming chromatin balls with perinuclear chromatolysis and small-sized degenerated mitochondria and disruption and loss of myofibrils and swollen mitochondria, which were in line with the electron microscopic results were done by Helal et al. (2020) that revealed severely damaged pleomorphic and disorganized mitochondria amongst myofibrils with malformed cristae, irregularly indented nuclei, and lysis of myofibrils.

All the present histological findings were in concurrence with studies that attributed CP cardiotoxicity to the inhibition of Na+/K+ ATPase and the disruption of calcium homeostasis leading to mitochondrial swelling as a result of intracellular sodium buildup (Iqubal et al., 2019) and OH-free radical generation by CP metabolism (Bhatt et al., 2017).

Moreover, light microscopic analysis of leukocytic infiltration in the study supported a report by Kurauchi et al. (2017) that CP activates cytokine production that regulates leukocyte traffic.

Cardiac muscle α-SMA-stained sections in the CP group were consistent with Kashef and Elswaidy (2022). Such a result was consistent with the justification that the healing of dead myocardial fibers began with an unchecked proliferation of extracellular matrix proteins that were abundantly generated by cardiac fibroblasts, causing

healing of the injury and fibrosis (El-Kader, 2020). These myofibroblasts meet the same standards as fibrocytes and muscle cells, allowing α-SMA to evaluate their composition and proliferation in the myocardium (Gava et al., 2016).

Bcl2-stained cardiac muscle sections of the CP group in the present study showed decreased brown coloration of sarcoplasm, indicating a very weak cytoplasmic reaction and the area of BCL2 immunoreactivity in groups II and III illustrated a significant decrease compared to the control group. These findings were in correspondence with those of Helal et al. (2020), who confirmed apoptosis in all rats injected with CP by positive immunoreactivity for caspase 3. Todorova et al. (2009) established that the etiological pathways causing CP-induced heart damage include both necrosis and apoptosis.

The results of the withdrawal group were nearly identical to those of the CP group, and there was no significant statistical difference in the examined parameters between the two groups, proving that CP withdrawal had no positive impact.

In the present work, we looked into the potential cardioprotective properties of Mangiferin in the context of CP-induced cardiotoxicity.

In our study, the mean serum levels of CK-MB and LDH in the CP plus Mangiferin group significantly declined compared to the CP group. This was in agreement with the findings of Bhatt et al. (2017) pointing out that the decrease in these biomarker enzyme levels to xanthone's reparative or membrane-stabilizing properties prevented further cardiac injury.

The H&E-stained sections of the CP plus Mangiferin group exhibited features nearly similar to those of the control group. While some muscle fibers with vacuolated sarcoplasm were separated by slightly dilated but not congested blood capillaries, a few pyknotic nuclei were also observed. Masson's stained sections illustrated a moderate amount of collagen fibers in-between the muscle fibers and around blood vessels, with a significant decline in the area of collagen deposition compared to groups II and III. Additionally, ultrathin images revealed the nearly normal structure of cardiac myocytes with a normal arrangement of myofibrils, but there were some degenerated myofibrils with mildly dilated T tubules and mild nuclear irregularity. Some degenerated mitochondria were noticed in the presence of lysosomes. Histological and ultrathin images of the CP plus Mangiferin group were consistent with those of Bhatt et al. (2017), who revealed that Mangiferin reverses toxic alterations caused by CP such as cardiomyocyte vacuolization, inflammatory cell infiltration, myocardial tissue separation, and myofibril loss.

In addition, increased brown coloration of sarcoplasm that indicates a positive cytoplasmic reaction, with a significant rise in area% of BCL2 in the CP plus Mangiferin group when compared to groups (II and III), coincided with Chen et al. (2021), who found that Mangiferin treatment lowers cardiomyocyte apoptosis while maintaining cardiac function. They also showed that administering mangiferin to treat MI effectively targets apoptotic cell death.

The bioactivity of Mangiferin was attributed to its capacity to prevent tissue damage by lowering localized O2 content and generating phenoxy radicals and metal-ligand complexes with iron that inhibit the formation of oxo-ferryl and OH radicals. Additionally, it protects healthy cellular function by maintaining the required oxidant-antioxidant balance and anti-inflammatory properties (Jiang et al., 2020).

Stem cells implanted into injured tissue were believed to encourage the development of new, functioning tissues and generate substances that reduce inflammation, promote the development of novel blood vessels, and inhibit cell senescence and hypertrophy (Sun et al., 2016).

The CP plus BM-MSCs group histological sections displayed features approximately similar to those of the control group, with a minimal amount of collagen fibers in between the muscle fibers and around blood vessels. But there was a slight separation of some fiber bundles. Also, there was minimal α-SMA expression in the present study. The presence of lysosomes and the rarefaction of sarcoplasm in ultrathin sections were noticed. These findings are consistent with a work by Helal et al. (2020) that demonstrated the therapeutic effectiveness of BM-MSCs in the form of an almost regular myocardial histological architecture that included regular muscle fiber arrangement with slight spacing. Few myocardial cells exhibited focal sarcoplasmic vacuolation. Euchromatic nucleus with minimally irregular contour and regular mitochondria distributed between myofibrils. Moreover, there was only a slight buildup of collagen fibers between the heart muscles. Also, the mean area percent of the collagen in MSC-treated group was significantly minimal in comparison to CP-treated rats.

The MSCs have paracrine anti-fibrotic activities to reduce ventricular rebuilding by controlling the proliferation of cardiac fibroblasts. This was how the quantity of fibrosis decreased following the injection of MSCs (Wysoczynski and Bolli, 2020).

In harmony with Tuby et al. (2013), the modest separation of some fiber bundles by extravasated RBCs in his work can be justified by the arrangement of newly produced contractile myofilaments in the cardiac cell cytoplasm at various stages of maturation, mimicking the morphological features of mature intact cardiomyocytes.

Moreover, the strong positive Bcl2 cytoplasmic reaction of the CP plus BM-MSCs group in this study is in line with Helal et al. (2020), who claimed that the MSC-treated CP cardiotoxicity group had a notable reduction in the caspase-3 reaction. Also, Ji et al. (2013) reported that, after an infarction, transplanting autologous undifferentiated mesenchymal stem cells may be a useful technique for myocardial regeneration, decreasing fibrosis and apoptosis while enhancing myocardial thickness.

The MSCs were thought to reduce the own-inflammatory response and boost the anti-inflammatory response by controlling immunocytes' proliferation and differentiation, according to Rog-Zielinska et al. (2016).

Despite the advantages of MSCs, the clinical use of MSC-based therapy is constrained. The limited vitality of the transplanted cells in the myocardium is responsible for this restriction. The proper management of the destiny and purpose of the engrafted cells is essential for the effectiveness of cell treatments. In light of this, methods for improving stem cell longevity, proliferation, and differentiation have emerged as one of the most popular areas of focus. Adjuvant medication use is a promising strategy for assisting stem cell therapy (Liu et al., 2014).

In the CP plus Mangiferin and BM-MSCs group, in this study, we explored the enhancement effects of Mangiferin on the therapeutic efficacy of BM-MSCs on CP-induced cardiac toxicity in adult albino male rat models. We deduced a significant decline in serum levels of CK-MB, LDH, and tissue

levels of MDA. In addition, H&E-stained sections demonstrated features similar to those of the control group. Masson's stained section revealed a very small amount of collagen fibers in between the muscle fibers; ultrathin sections demonstrated cardio myocytes similar to the control group. Also, there was a very minimal α-SMA expression and a strong positive Bcl2 cytoplasmic reaction.

Finally, the fact that the CP plus Mangiferin and BM-MSCs group displayed a non-significant difference when compared to the control group indicated the extreme improvement in all examined cardiac parameters when Mangiferin was added to BM-MSCs.

Conclusion

Cyclophosphamide-induced myocardial damage, fibrosis, and apoptosis can be significantly avoided by Mangiferin or BM-MSCs. These findings are crucial for cancer patients who are experiencing CP-induced cardiac problems. However, treating the CP-induced cardiotoxicity rat model with Mangiferin and BM-MSCs simultaneously improves all histological, ultrastructural, and immune-histochemical cardiac parameters superior to their application separately. These findings point to a unique pharmacological strategy for enhancing the effectiveness of MSC-based therapies for cardiovascular disorders.

Conflicts of Interest

There were no declared conflicts of interest that would have affected this article.

References

Afzal, M.R., Samanta, A., Shah, Z.I., et al. (2015) 'Adult bone marrow cell therapy for ischemic heart disease: evidence and insights from randomized controlled trials`. *Circ. Res.,* 117(6), pp. 558-575.

Akter, S., Moni, A., Faisal, G.M., et al. (2022) 'Renoprotective effects of Mangiferin: pharmacological advances and future perspectives`. *Int. J. Environ. Res. Public Health*, 19(3), pp. 1864.

Ayza, M.A., Zewdie, K.A., Tesfaye, B.A., et al. (2020) 'The role of antioxidants in ameliorating cyclophosphamide-induced cardiotoxicity`. *Oxidative Medicine and Cellular Longevity*,10: 4965171.

Bhatt, L., Sebastian, B. and Joshi, V. (2017) 'Mangiferin protects rat myocardial tissue against cyclophosphamide-induced cardiotoxicity`. *J. Ayurveda Integr. Med.*, 8 (2), pp. 62-67.

Chen, L., Li, S., Zhu, J., et al. (2021) 'Mangiferin prevents myocardial infarction-induced apoptosis and heart failure in mice by activating the Sirt1/FoxO3a pathway`. *J. Cell. Mol. Med.*, 25(6), pp. 2944-2955.

Du, S., Liu, H., Lei, T., et al. (2018) 'Mangiferin: An effective therapeutic agent against several disorders (Review)`. *Mol. Med. Rep.*, 18, pp. 4775-4786.

Dykstra, M.J. and Reuss, L.E. (2003). *Staining methods for semithins and ultrathins. In: Biological electron microscopy, theory, techniques, and troubleshooting*. 2nd ed., Kluwer

Academic Publishers/ Plenum Publishers, pp.175-196.

El-kader, A. (2020) 'Evaluation of azithromycin-induced cardiotoxicity in male albino rats and the possible protective role of nigella sativa oil`. *Egyptian Journal of Histology*, 43(2), pp. 465-476.

Emeka, P.M., Morsy, M.A., Alhaider, I.A. and Chohan, M.S. (2021) 'Protective effect of caffeic acid phenethyl ester against acute and subchronic mice cardiotoxicity induced by cyclo-phosphamide alone or plus naproxen`. *Pharmacognosy Magazine*, 16 (71), pp. 585-591.

Gava, F., Silva, S., Rosa, F., et al. (2016) 'Correlation between systolic function and presence of myofibroblasts in doxorubicin-induced cardio-myopathy`.*Ciência Rural*, 46 (9), pp.1642-1648.

Guan, W., Liu, Y., Liu, Y., et al. (2019) 'Proteomics research on the protective effect of mangiferin on H9C2 cell injury induced by H2O2`. *Molecules*, 24:pp.1911.

He, W., You, Y., Du, S., et al. (2019) 'Anti-neoplastic effect of mangiferin on human ovarian adenocarcinoma OVCAR8 cells via the regulation of YAP`. *Oncol. Lett.*, 17(1), pp. 1008-1018.

Helal, A. I., Helal, O., Metwaly, H., et al. (2020) 'Histological and immune-histochemical study on the possible therapeutic role of stem cells and curcumin in cyclophosphamide-induced cardiotoxicity in adult male albino rat`. *Benha Medical Journal*, *37*(1), pp. 193-206.

Iqubal, A., Iqubal, M. K., Sharma, S., et al. (2019) 'Molecular mechanism involved in cyclophosphamide-induced cardiotoxicity: an old drug with a new vision`. *Life Sciences, 218,* pp. 112-131.

Ji, L., Long, X. and Tian, H. (2013) 'Effect of transplantation of bone marrow stem cells on myocardial infarction size in a rabbit model`. *World J. Emerg . Med.*, 4(4), pp. 304-310.

Jiang, T., Han, F., Gao, G. and Liu, M. (2020) ' Mangiferin exert cardio-protective and anti-apoptotic effects in heart failure induced rats`. *Life Sci.*, 249: pp. 117476.

Kashef, S.M. and Elswaidy, N.R. (2022) 'The possible role of allicin in ameliorating azithromycin induced cardiotoxicity in adult male albino rat: A histological and immune-histochemical study`. *Egyptian Journal of Histology*, 45(3), pp. 863-874.

Katayama, M., Imai, Y., Hashimoto, H., et al. (2009) 'Fulminant fatal cardiotoxicity following cyclo-phosphamide therapy`. *Journal of Cardiology*, *54*(2), pp. 330-334.

Kim, J. and Chan, J. J. (2017) ' Cyclophosphamide in dermatology`. *Australasian Journal of Dermatology, 58(1), pp.* 5-17.

Kurauchi, K., Nishikawa, T., Miyahara, E., et al. (2017) 'Role of metabolites of cyclophosphamide in cardiotoxicity`. *BMC. Research Notes,* 10 (1) pp. 406.

Liao, S., Zhang, Y., Ting, S. and Zhen, Z. (2019) 'Potent immune-modulation and angiogenic effects of mesenchymal stem cells versus cardiomyocytes derived from

pluripotent stem cells for treatment of heart failure`. *Stem Cell Research & Therapy,* 10(1), pp. 78.

Liu, J., Wang, H. and Wang, Y. (2014) 'The stem cell adjuvant with Exendin-4 repairs the heart after myocardial infarction via STAT3 activation`. *J. Cell. Mol. Med.,* 18(7), pp. 1381-1391.

Liu, Y., Tan, D., Shi, L., et al. (2015) 'Blueberry anthocyanins-enriched extracts attenuate cyclophosphamide-induced cardiac injury`. *PLOS ONE,* 10(7): e0127813.

Luo, L., Tang, J., Nishi, K., et al. (2017) 'Fabrication of synthetic mesenchymal stem cells for the treatment of acute myocardial infarction in mice`. *Circ. Res.,* 120, pp. 1768-1775.

Prado, Y., Rodeiro, I., Merino, N. and Delgado, R. (2015) 'Acute and 28-day subchronic toxicity studies of mangiferin, a glucosyl xanthone isolated from Mangifera indica L. stem bark`. *Journal of Pharmacy & Pharmacognosy Research*, *3*(1), pp. 13-23.

Ranchoux, B., Günther, S., Quarck, R., et al. (2015) 'Chemotherapy induced pulmonary hypertension: role of alkylating agents`. *The American Journal of Pathology, 185(2), pp.* 356-371.

Ren, H., Sang, Y., Zhang, F., et al. (2016) 'Comparative analysis of human mesenchymal stem cells from umbilical cord, dental pulp, and menstrual blood as sources for cell therapy`. *Stem Cells Int., 2016:*3516574.

Rog-Zielinska, E. A., Norris, R. A., Kohl, P. and Markwald, R. (2016) 'The living scar–cardiac fibroblasts and the injured heart`. *Trends in Molecular Medicine,* 22(2), pp. 99 -114.

Ruiz-Larnea, M. B., Leal, A. M., Liza, M., et al. (1994) 'Antioxidant effects of estradiol and 2-hydroxyestradiol on iron-induced lipid peroxidation of rat liver microsome`.*Steroid,* 59(6), pp. 383-388.

Sadhukhan, P., Saha, S., Dutta, S. and Sil, P. C. (2018) 'Mangiferin ameliorates Cisplatin induced acute kidney injury by upregulating Nrf-2 via the activation of PI3K and exhibits synergistic anticancer activity with Cisplatin`. *Front. Pharmacol.,* 9*:* pp. 638.

Safdar, M. N., Kausar, T., Nadeem, M., et al. (2017) 'Cardioprotective effect of mango and kinnow peel extracts on doxorubicin-induced cardiotoxicity in albino rats`. *Proceedings of the Pakistan Academy of Sciences,* 54(3), pp. 219-235.

Shanmugarajan, T. S., Arunsundar, M., Somasundaram, I., et al. (2008) 'Cardioprotective effect of Ficus hispida Linn. on cyclophosphamide provoked oxidative myocardial injury in a rat model`. *International Journal of Pharmacology,* 4(2), pp. 78-87.

Short, B. and Wagey, R. (2013) 'Isolation and culture of mesenchymal stem cells from mouse compact bone`. *Methods. Mol. Biol.,* 946, pp. 335-347.

Suchal, K., Malik, S., Khan, S. I., et al. (2017) 'Protective effect of mangiferin on myocardial ischemia-reperfusion injury in streptozotocin-induced diabetic rats: role of AGE-RAGE/MAPK pathways`. *Sci Rep, 7:* 42027.

Sun, R., Li, X., Liu, M., et al. (2016) 'Advances in stem cell therapy for cardiovascular disease`. *Int. J. Mol. Med., 38(1), pp.* 23-29.

Sun, S. J., Lai, W. H., Jiang, Y., et al. (2021) 'Immunomodulation by systemic administration of human-induced pluripotent stem cell derived mesenchymal stromal cells to enhance the therapeutic efficacy of cell-based therapy for treatment of myocardial infarction`. *Theranostics,* 11(4), pp. 1641-1654.

Suvarna, K., Layton, C., & Bancroft, J. (2018) '*The Hematoxylin and eosin, Connective and mesenchymal tissues with their stains, Immuno-histochemical techniques and Transmission electron microscopy*`. In: Bancroft's Theory and practice of Histological Techniques ¨. (8th ed.) Churchill Livingstone Elsevier, Oxford, pp. 173-493.

Thomas, L. (1998) '*Clinical Laboratory Diagnostics: Use and Assessment of Clinical Laboratory Results*`. (1st ed.) TH-Books Verlagsgesellschaft, Frankfurt, Germany.

Thomford, N. E., Senthebane, D. A., Rowe, A., et al. (2018) 'Natural products for drug discovery in the 21st century: Innovations for novel drug discovery`. *Int. J. Mol. Sci.,* 19, pp. 1578.

Todorova, V., Vanderpool, D., Blossom, S., et al. (2009) 'Oral glutamine protects against cyclophosphamide-induced cardiotoxicity in experimental rats through increase of cardiac glutathione`. *Nutrition,* 25(7-8), pp. 812-817.

Traverse, J. H., Henry, T. D., Ellis, S. G., et al. (2011) ' Effect of intracoronary delivery of autologous bone marrow mononuclear cells 2 to 3 weeks following acute myocardial infarction on left ventricular function: The LateTIME randomized trial`. *JAMA,* 306(19), pp. 2110-2119.

Tuby, H., Yaakobi, T. and Maltz, L. (2013) 'Effect of autologous mesenchymal stem cells induced by low level laser therapy on cardiogenesis in the infarcted area following myocardial infarction in rats`. *J. Biomed. Science and Engineering,* 6(8A), pp. 24-31.

Wysoczynski, M. and Bolli, R. (2020) 'A realistic appraisal of the use of embryonic stem cell-based therapies for cardiac repair`. *Eur. Heart J.,* 41(25), pp. 2397-2404.

Zaghloul, S., Abou Elnour, R., Abdelfattah, M., and Ismail, D. (2020) 'Comparative histological study on the effect of mesenchymal stem cell and losartan on cardiac injury induced by doxorubicin in male albino rats`. *Egyptian Journal of Histology,* 42(4), pp. 815-825.

مانـجيفيرين يعزز الفعالية العلاجية للخلايا الجذعية للنخاع العظمي على السمية القلبية المستحثة بسيكلوفوسفاميد في نماذج ذكور الفئران البيضاء البالغة

مي حسن ابراهيم[١] ، رشا ممدوح سلامة[٢]

[١] قسم التشريح والأجنة ، كلية الطب البشرى، جامعة بنها
[٢] قسم التشريح والأجنة، كلية الطب البشرى، جامعة المنوفية

يعاني ما بين ٧ - ٢٨% من المرضى الذين يتلقون سيكلوفوسفاميد من تسمم القلب. تهدف هذه الدراسة إلى معرفة المزيد عن التأثيرات المعززة للمانجيفيرين على الفعالية العلاجية للخلايا الجذعية الوسيطة لنخاع العظم على سمية القلب الناجمة عن السيكلوفوسفاميد في نماذج الفئران البيضاء البالغة. تم فصل تسعين من الفئران البيضاء الذكور إلى ست مجموعات؛ المجموعة الضابطة ، المجموعة المعالجة بالسيكلوفوسفاميد ، مجموعة الانسحاب، مجموعة سيكلوفوسفاميد بالإضافة إلى المانجيفيرين ، مجموعة سيكلوفوسفاميد بالإضافة إلى الخلايا الجذعية للنخاع العظمي ، مجموعة سيكلوفوسفاميد بالإضافة إلى مانجيفيرين والخلايا الجذعية للنخاع العظمي .عندما تم فحص عضلة القلب لمجموعة السيكلوفوسفاميد تحت المجهر، ظهرت ألياف عضلة القلب مفرغة مع ارتشاح خلايا أحادية النواة بين الألياف. أيضًا، لوحظ تفكك الليفات العضلية، واتساع فى الشبكة الاندوبلازمية الملساء، والميتوكوندريا المتدهورة من خلال الميكروسكوب الالكترونى. أظهرت بعض الأنوية تعاني تحلل لوني، في حين كان البعض الآخر متغاير اللون مع عدم انتظام فى غشاء النواة. تم التحقق من صحة هذه النتائج من خلال زيادة كبيرة في α-SMA وانخفاض كبير فيBcl-2 ، وكذلك زيادة واضحة في ترسب ألياف الكولاجين، بالإضافة إلى ذلك تم تأكيدها من خلال النتائج البيوكيميائية في شكل ارتفاع مستويات CK-MBو LDH فى مصل الدم ومستوى MDA فى النسيج . كانت نتائج مجموعة الانسحاب تشبه نتائج مجموعة السيكلوفوسفاميد .تم تحسين بنية عضلة القلب ، وترسب ألياف الكولاجين، ومستويات CK-MBو LDH فى مصل الدم ومستوى MDA فى النسيج فى مجموعات سيكلوفوسفاميد بالإضافة إلى المانجيفيرين و مجموعة سيكلوفوسفاميد بالإضافة إلى الخلايا الجذعية للنخاع العظمي ، ولكنها لم تحقق بعد التحسن الكامل في الأنسجة، والبنية التحتية، والكيمياء المناعية، و معلمات القلب البيوكيميائية. مؤخرا حققت مجموعة سيكلوفوسفاميد بالإضافة إلى مانجيفيرين والخلايا الجذعية للنخاع العظمي نتائج مشابهة إلى حد كبير للمجموعة الضابطة.